

Characterisation of the field-saturated hydraulic conductivity on a hillslope: in situ single ring pressure infiltrometer measurements

J. Mertens^{a,*}, D. Jacques^b, J. Vanderborght^c, J. Feyen^a

^aLaboratory of Soil and Water, Faculty of Agricultural and Applied Biological Sciences, Katholieke Universitat Leuven, Vital Decosterstraat 102, B-3000 Leuven, Belgium

^bSCK-CEN, Boeretang 200, B-2400 Mol, Belgium

^cForschungszentrum Jülich, D-52425 Jülich, Germany

Received 23 May 2001; revised 8 December 2001; accepted 1 March 2002

Abstract

Spatial variability of surface hydraulic properties is an important factor for infiltration and runoff processes in agricultural fields. At 120 locations on a hillslope, steady-state infiltration rates were measured at two applied pressure heads with a single-ring infiltrometer. The solution of two steady-state infiltration equations for each location (the simultaneous-equation approach, SEA) yielded 41 negative α -values, 79 positive α values and 120 positive K_{fs} -values. The sensitivity of K_{fs} and α to small measurement errors was estimated using a Monte-Carlo simulation (MC). Results of this MC simulation showed that the uncertainty on α is extremely high while the uncertainty on K_{fs} is fairly small. Hence, although the pressure infiltrometer technique as applied here is useful to estimate K_{fs} at each measurement location, it is not suited for the estimation of an α -value at each measurement location. A new procedure is proposed for the simultaneous estimation of one overall 'field α ' and the 79 K_{fs} values of measurement locations having a positively calculated α using SEA. Using this field α , K_{fs} values for the other 79 locations with a negative α are hence determined. Finally, the spatial correlation of K_{fs} on the hillslope is examined. Ranges of $\ln(K_{fs})$ between 2.85 and 3.8 m were observed, respectively, for the omnidirectional case and the y direction along the hillslope μ . © 2002 Elsevier Science B.V. All rights reserved.

Keywords: Hydraulic conductivity; Hillslope; Inverse parameter estimation; Sensitivity analysis; Spatial variability

1. Introduction

Field investigations of the hydraulic properties of the unsaturated (vadose) zone are becoming increasingly important elements in hydrogeological and geotechnical studies. The properties of the unsaturated zone control the generally slow downward seepage of potential ground water contaminants as

well as the amount of direct runoff (Elrick et al., 1989). A number of field techniques have been used to measure the hydraulic properties of soils in the unsaturated zone (Angulo-Jaramillo et al., 2000). Infiltration based methods are recognised as valuable tools to investigate hydraulic and transport soil properties. In particular, three complementary methods appear to be interesting in the study of unsaturated and-near saturated hydrological soil behaviour. They are the confined one-dimensional pressure double ring infiltrometer, the unconfined three-dimensional single ring pressure infiltrometer and the unconfined three-dimensional tension disc infiltrometer methods.

* Corresponding author. Tel.: +32-16-32-97-21; fax: +32-16-32-97-60.

E-mail address: jan.mertens@agr.kuleuven.ac.be (J. Mertens).

In this study we examine infiltration data measured with a constant head single-ring pressure infiltrometer method. This technique is useful in the estimation of the in situ K_{fs} [LT^{-1}] ('field-saturated' hydraulic conductivity) and ϕ_m [L^2T^{-1}] (matric flux potential). The term field-saturated is used because, under field conditions, a certain amount of air is usually entrapped in the soil during the infiltration process (Reynolds et al., 1983; Elrick et al., 1989). This can result in lower estimates of the 'saturated' hydraulic conductivity compared to measurements in completely saturated soils (Stephens et al., 1987).

The flux potential, ϕ_m , is defined as (Gardner, 1958):

$$\phi_m = \int_{h_i}^0 K(h)dh \quad (1)$$

where h is the soil pressure head and h_i the initial soil pressure head [L]. ϕ_m is independent of the applied head for the pressure infiltrometer method and is related to α [L^{-1}]:

$$\alpha = \frac{K_{fs}}{\phi_m} \quad (2)$$

The α parameter is a measure of the relative contributions of gravity and capillary forces to water movement in an unsaturated soil. The smaller the α value, the larger the capillary forces relative to gravity. The value of α measured in the field using ponded infiltration techniques is determined primarily by soil structure, particularly when macropores are present (Elrick et al., 1989, 1995).

Constant head conditions have traditionally been used because constant head devices are easy to maintain experimentally and because the analysis is relatively simple. A difficulty with this approach is that insufficient information is obtained from the measurement of steady state flow under one constant head to evaluate both K_{fs} and ϕ_m (Elrick et al., 1995). Either one of the two parameters (or the α -value), must be measured or estimated independently (Elrick et al., 1989) or steady state flow measurements are needed for two or more ponded heads. If α is estimated independently however, some error can result. If steady state measurements are taken at two or more heads, soil heterogeneity can cause a large percentage of invalid (i.e. negative) and unrealistic K_{fs} and ϕ_m values (Elrick et al., 1995).

The fixed α value approach as suggested by Elrick et al. (1989), requires only one flow rate measurement. However, individual α -values for soils are generally not available. Based on structural and textural information, Elrick et al. (1989) classified soils into four categories and suggested choices of α for each category. They proposed values of α ranging between 0.01 cm^{-1} (compacted clays e.g. landfill caps and liners, lacustrine or marine sediments, etc.) and 0.36 cm^{-1} (coarse and gravely sands; may also include some highly structured soils with large cracks and macropores).

In this study, only constant head infiltration measurements were performed for two heads at each measurement location. This was done because of the simplicity of measuring the infiltration and because of the belief that the procedure presented in this study allows the achievement of good estimates of K_{fs} . K_{fs} and α are calculated from the observed infiltration rates (Q_1 and Q_2 [LT^{-1}]) corresponding to the applied heads (h_1 and h_2 [L]) using the classical constant head approach (or simultaneous-equations approach, SEA) (Reynolds and Elrick, 1990). Philip (1985) concluded that negative values of K_{fs} and α imply that solutions for K_{fs} and α are too strongly dependent on the ratio of the observed infiltration rates (Q_2/Q_1). He gave two numerical examples how a random measurement error and some mild heterogeneity could cause negative K_{fs} or α estimates. Elrick et al. (1989) report three error sources that could cause negative K_{fs} or α when using Guelph permeameter method: (i) non-attainment of true steady-state flow; (ii) errors in the experimental measurements of Q_1 and Q_2 because of air bubble size and reading errors in the permeameter; and (iii) entrapment of air in the soil due to water redistribution during filling of the permeameters and restarting of infiltration. These three error sources exist also for the single-ring pressure infiltrometer measurements since the only difference is the borehole and its preparation. We minimised these error sources during measurements by (i) increasing measurement time, (ii) using small air inlet tubing and (iii) making the reservoir large enough to make measurements at two heads possible without refilling (Ankeny et al., 1988). Nevertheless K_{fs} and α are very sensitive to the Q_2/Q_1 ratio (Wu et al., 1993). Preferential flow in macropores (vertical and lateral cylindrical pores, cracks) not activated in one infiltration measurement at a

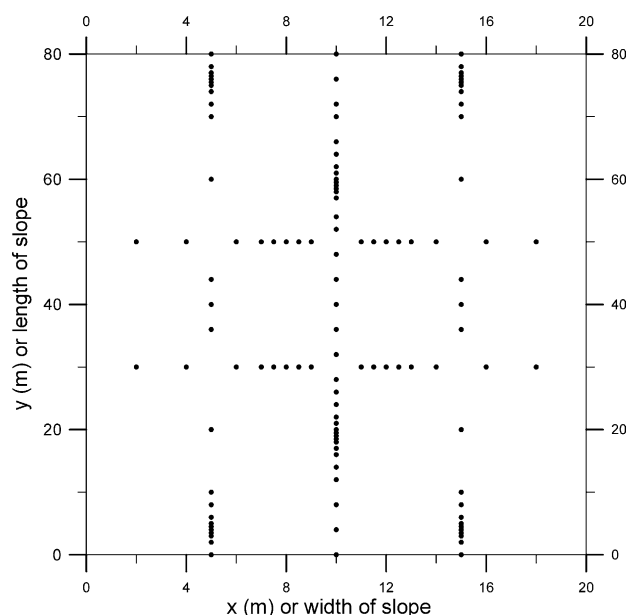


Fig. 1. A scheme of the hillslope showing the 120 measurement locations.

specific head becomes activated in the other infiltration measurement with the second applied head, can change the Q_2/Q_1 ratio, depending on the geometrics and locations of the macropores. The activation are not of macropore flow depending on the potential is well known in the unsaturated domain (Elrick and Reynolds, 1992). In the ideal case where macropores would be homogeneously spread out over the soil volume, no artefacts can be encountered. When the saturated bulb is so small that no macropores are within the bulb for the smaller pressure head but are in the saturated bulb for the subsequently applied pressure head, the flow may increase dramatically due to the expansion of the bulb and the activation of macropores.

The objectives of this research were to: (i) examine the possibilities of single-ring pressure infiltrometer measurements in estimating that K_{fs} and α using the classical constant head approach for two heads at each measurement location, (ii) study the sensitivity of K_{fs} and α to small measurement errors, (iii) develop a procedure for the estimation of one overall 'field α ' using an inverse optimisation technique and (iv) estimate the spatial correlation scale of K_{fs} measured on a hillslope.

2. Materials and methods

2.1. Site description

We measured infiltration using single-ring pressure infiltrometers at 120 locations on a $80 \times 20 \text{ m}^2$ field plot located on a hillslope with a sandy-loam soil texture (Luvisol) in Rillaar, Belgium. The selected plot is located in a fruit tree research area. Before September 1999, the plot was covered with apple trees for 14 years. In September 1999, the apple trees were removed and the site was covered with grass ever since. The hillslope has a mean slope of 10% and is currently in use as an experimental plot for a rainfall–runoff study. The pressure infiltrometer measurements were done in August 2000 in the context of this hillslope rainfall–runoff study.

2.2. Measurements

To estimate field-saturated conductivity (K_{fs}), we measured the steady-state infiltration rate from a ring under a constant positive pressure head (H) using a single-ring pressure infiltrometer. Water is supplied to the soil surface at a positive head through a sealed top lid by a Mariotte bottle with a moveable

air tube allowing a wide range of H . The set-up is similar to the Guelph Permeameter reservoir (Reynolds et al., 1985; Reynolds and Elrick, 1990; Vauclin et al., 1994; Angulo-Jaramillo et al., 2000). The ring has a diameter of 95 mm and can be driven into the ground to a maximum depth of 57 mm. The ring was carefully driven into the ground without removing the short grass; no special surface preparation was needed. The grass was not removed as we were interested in the in situ natural infiltration characteristics. At each location, steady state infiltration rates were measured manually at two different pressure heads applied in a sequence at a single location. The supplied pressure heads were slightly different for each location, but in all cases, the measurements started at the smallest value. The supplied pressure heads ranged from +6 cm to a maximum of +25 cm. Steady state was reached after an average of 90 min per head. The criterion used for attaining steady-state infiltration was that the 5 min infiltration volume during a 30 min record remained constant. All measurements were done during a long dry period since the initial water content of the soil may influence the estimation of K_{fs} (Bagarello and Provenza, 1996). The measurement campaign was limited in time thereby minimising the risk of temporal changes in soil structure that may affect the saturated conductivity (Russo et al., 1997). In this case, no prior rainfall–runoff experiments were performed and the measurement campaign was 2 weeks long. No precipitation was recorded during that period.

The total number of measurement locations was 120 and the measurement scheme is shown in Fig. 1. The scheme layout was designed in order to obtain enough pairs for the estimation of semi-variograms at different lag distances in both the x - and y -direction. An accurate estimation of the semi-variograms requires a minimum of 30–50 pairs (Journal and Huijbregts, 1978). To estimate directional variograms, measurements were done on lines parallel and perpendicular to the hillslope. The testing of the layout was performed using the GSLIB program (Deutsch and Journal, 1992).

3. Derivation of K_{fs} and α

3.1. Simultaneous-equations approach

An analysis of steady, ponded infiltration from a

single ring which takes into account the soil hydraulic parameters, ring radius, depth of ring insertions, and depth of ponding was published by Reynolds and Elrick (1990). The following equation for three-dimensional steady flow of water from the ring was given:

$$q_{0\infty} = K_{fs} \left(1 + \frac{H}{\pi r_d G} \right) + \frac{\phi_m}{\pi r_d G} \quad (3)$$

where $q_{0\infty}$ (LT^{-1}) is the steady flow rate, K_{fs} (LT^{-1}) the field-saturated hydraulic conductivity, H (L) the height of the ponded head, r_d (L) the ring radius, ϕ_m (L^2T^{-1}) the matric flux potential and G (–) a dimensionless parameter:

$$G = 0.316 \frac{d}{r_d} + 0.184 \quad (4)$$

where d (L) is the depth of insertion of the ring in the soil. The first term in the right-hand side of Eq. (3) represents the gravitational effect, the second one corresponds to the influence of the ponded head, H , and the third term represents the contribution of the capillary forces to the soil water flow (Angulo-Jaramillo et al., 2000). When the steady-state infiltration rates are measured at two positive hydraulic heads H_1 and H_2 at the same location, K_{fs} and ϕ_m are obtained by solving the resulting two Eqs. (3) and (4) (SEA approach). On each measurement location, two hydraulic heads were supplied and the corresponding steady state infiltration rate measured. This allows the simultaneous solving of Eqs. (3) and (4) for K_{fs} and ϕ_m (or α) per measurement location.

3.2. Sensitivity analysis

A rigorous analysis of the uncertainties of the single-ring pressure infiltrometer measurements is beyond the scope of this study. Instead, a simple error analysis using Monte-Carlo simulations (MC simulations) was performed here to assess the propagation of uncertainties in measured inflow rates on the values of K_{fs} and α . A random error on the steady state infiltration rate is assumed. The error is assumed equivalent to a possible reading-off error of mean 0 mm and standard deviation 0.5 mm (normal distribution) on the value read-off the reservoir. The error is randomly added to read-off values for both applied pressure heads. Inflow rates (Q_1 and Q_2) are calculated

and the assumed error in this experiment results in a standard deviation on Q_1 and Q_2 of $0.0034 \text{ cm min}^{-1}$. Mean of Q_1 and Q_2 over all measurements is 0.2 cm min^{-1} so the mean error on the inflow rates is about 1.7%. Consequently K_{fs} and α values are calculated using the SEA for each random error. Thousand simulations per measurement location or 120 000 simulations were performed and the statistical properties deduced.

A second sensitivity analysis is performed in order to examine the effect of an increase in the number of pressure head levels per location on the uncertainty of K_{fs} and α . This analysis is done for three pressure heads and the corresponding infiltration rate per measurement location is measured. MC simulations were performed using the same probability distribution on the inflow rate as described earlier, but assuming three pressure head levels. Three K_{fs} values ($0.005, 0.03, \text{ and } 0.09 \text{ cm min}^{-1}$) and six α values ($0.01, 0.02, 0.05, 0.1, 0.2, \text{ and } 0.5 \text{ cm}^{-1}$) are arbitrarily chosen though keeping in mind the range of α proposed by Elrick et al. (1989). For each pair of K_{fs} and α , three $q_{0\infty}$ values were calculated for three different H 's (10, 20 and 30 cm) using Eq. (3). Then a measurement error is added to $q_{0\infty}$ and a regression through the new $(H, q_{0\infty}^{\otimes})$ is performed ($q_{0\infty}^{\otimes}$: theoretical perturbed infiltration rate). Three pressure head levels require regression through the three pairs $(H, q_{0\infty}^{\otimes})$ while when using only two levels, simultaneously solving of Eq. (3) for both pairs was sufficient. Three pairs are hence expected to result in smaller standard deviations of K_{fs} and α but are more time consuming when the field measurements are taken into account.

3.3. Inverse optimisation technique

The calculation of best fit parameters (e.g. K_{fs} and α) in general requires minimisation of the following objective function (Bard, 1974):

$$SSR = \sum_{i=1}^n [F(p) - m_i]^2 \tag{5}$$

where SSR is the sum of squared residuals, $F(p)$ the model function with a set of parameters p , and m a vector of n data points.

We propose here a new procedure using an optimisation technique. The procedure optimises simul-

taneously one overall ‘field’ α and n K_{fs} values (one at each measurement location). The optimum is reached when the SSR is minimal i.e. when the sum of squared differences between observed Q and simulated $q_{0\infty}$ values for each location is minimal. Considering only one α , Eq. (3) can be rewritten as:

$$\begin{bmatrix} Q_{1,1} \\ Q_{1,2} \\ Q_{2,1} \\ Q_{2,2} \\ \vdots \\ Q_{n,1} \\ Q_{n,2} \end{bmatrix} = \begin{bmatrix} H_{1,1}00\dots0 \\ H_{1,2}00\dots0 \\ 0H_{2,1}00\dots0 \\ 0H_{2,1}00\dots0 \\ \vdots \\ 00\dots H_{n,1} \\ 00\dots H_{n,2} \end{bmatrix} \times \begin{bmatrix} a_1 \\ a_1 \\ a_2 \\ a_2 \\ \vdots \\ a_n \\ a_n \end{bmatrix} + \begin{bmatrix} 100\dots0 \\ 100\dots0 \\ 0100\dots0 \\ 0100\dots0 \\ \vdots \\ 00\dots1 \\ 00\dots1 \end{bmatrix} \tag{6}$$

$$\times \begin{bmatrix} a_1 \\ a_1 \\ a_2 \\ a_2 \\ \vdots \\ a_n \\ a_n \end{bmatrix} \times b$$

where $a_i = K_i/\pi r_d G$, $b = 1/\alpha + \pi r_d G$, $Q_{i,1}, Q_{i,2}$ and $H_{i,1}, H_{i,2}$ correspond, respectively, to the first and second measured steady state infiltration rate ($Q_{0\infty}$) and head (H) at each measurement location i .

Eq. (6) is the model with parameter a_i and b . Note that Eq. (6) is in fact a non-linear model because of the second term. Lower limits for K_{fs} and α were set to 0 while upper limits were set to infinity for all parameters. The initial estimates of K_{fs} were arbitrarily set at 0.25 cm min^{-1} and the initial estimate α was set at 0.01 cm^{-1} .

3.4. Statistical and geostatistical methods

Since only one field α value is considered in this study, only K_{fs} is considered in the analysis. Prior to the spatial analysis of K_{fs} , it is convenient to examine the data of K_{fs} by means of simple conventional

Table 1

Descriptive statistics of K_{fs} and α calculated using the SEA and in comparison with the statistics of the optimised values

	<i>N</i>	Avg.	Min.	Max.	Std Dev.
<i>All measurements (SEA)</i>					
K_{fs} (cm min ⁻¹)	120	0.0734	0.0010	1.4544	0.1555
α (1 cm ⁻¹)	120	-0.0126	-9.5796	8.2911	1.1739
<i>Location of positive α values (SEA)</i>					
K_{fs} (cm min ⁻¹)	79	0.0324	0.0010	0.1320	0.0350
α (1 cm ⁻¹)	79	0.1864	0.0006	8.2911	0.9298
<i>Location of negative α values (SEA)</i>					
K_{fs} (cm min ⁻¹)	41	0.1526	0.0051	1.4544	0.2445
α (1 cm ⁻¹)	41	-0.3958	-9.5796	-0.0249	1.4784
<i>All measurements (optimisation)</i>					
K_{fs} (cm min ⁻¹)	120	0.0293	0.0020	0.1516	0.0292
α_{opt} (1 cm ⁻¹)	1	0.03	/	/	/

statistical methods. The Lilliefors test (Conover, 1980) is used as normality check of $\ln K_{fs}$. The Lilliefors test is similar to the Kolmogorov–Smirnov test, but adjusts for the fact that the parameters of the normal distribution are estimated from the K_{fs} values rather than specified in advance. Using the theory of the regionalised variables (Cressie, 1993), the spatial correlation structure of K_{fs} is investigated. The semi-variance is defined as:

$$\gamma(h) = \frac{1}{2n(h)} \sum_{i=1}^{n(h)} [z(x_i) - z(x_i + h)]^2 \quad (7)$$

where $\gamma(h)$ is the estimated semi-variance for lag distances class h , $z(x_i)$ and $z(x_i + h)$ the measured sample values at point x_i and $x_i + h$, respectively, and $n(h)$ the total number of sample pairs for the interval h . The omnidirectional and directional variograms along x and y axes are calculated using the GSLIB program (Deutsch and Journal, 1992). An exponential model was visually fitted to the variograms:

$$\gamma(h) = C_0 + C_s[1 - e^{-3h/a}] \quad (8)$$

where C_0 is the nugget variance and C_s the (co)variance contribution or sill value, h the lag distance (m) and a the practical range, that is the distance at which the variogram value is 95% of the sill. The model was checked by cross-validation, testing for the absence of systematic errors and the consistency of the kriging variance and error. In particular, following Jury et al. (1987a,b) and Russo and Jury (1987a,b), we checked

the following criteria:

$$ME = \frac{1}{n} \sum_{i=1}^n RE(x_i) \cong 0 \quad (9)$$

where

$$RE = \frac{\hat{z}(x_i) - z(x_i)}{\{\text{var}[\hat{z}(x_i) - z(x_i)]\}^{1/2}} \quad (10)$$

and that

$$MRE = \left[\frac{1}{n} \sum_{i=1}^n RE(x_i)^2 \right]^{1/2} \cong 1 \quad (11)$$

where ME is the mean of the reduced error vector RE, MRE the mean square reduced error, n the sample size, $z(x_i)$ and $\hat{z}(x_i)$ the measured and predicted (krigged) values at location x_i , where i varies from 1 to n .

4. Results and discussion

4.1. Simultaneous-equations approach

As discussed earlier, an important limitation of the single-ring pressure infiltrometer measurements is the potential for negative values of the estimated K_{fs} and/or α (Heinen and Raats, 1990; Elrick and Reynolds, 1992; Wu et al., 1993; Russo et al., 1997). The SEA approach (Eqs. (3) and (4)) can only yield positive values for K_{fs} if $Q_2 > Q_1$, but can yield both positive

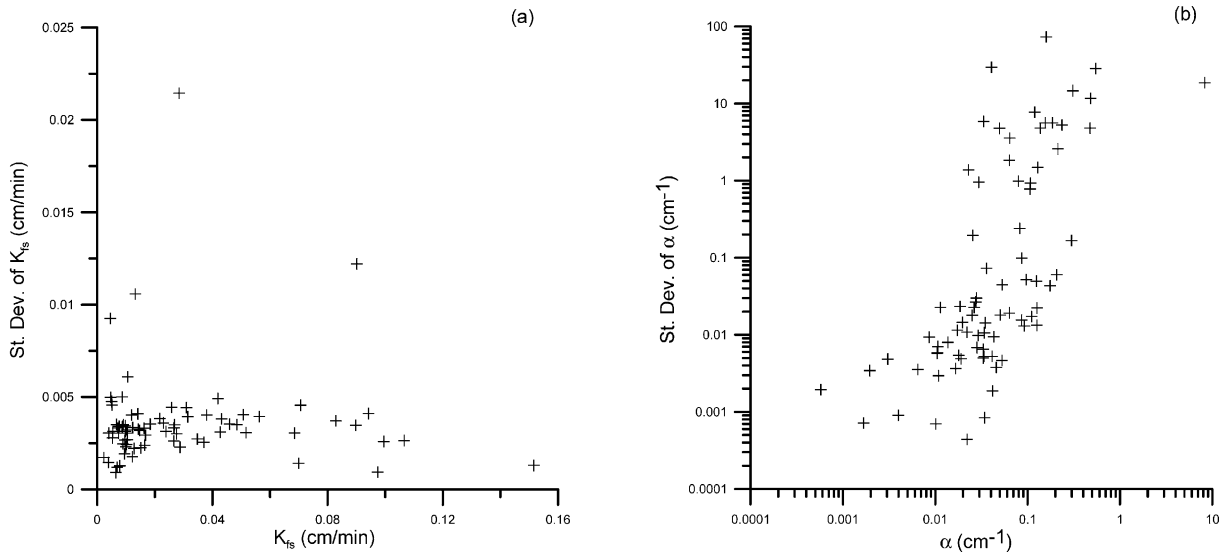


Fig. 2. Result of the MC simulations with two applied pressure heads. (a) K_{fs} and standard deviation of K_{fs} (b) α and standard deviation of α .

and negative values for α . That is why all 120 calculated K_{fs} values of our data set were found to be positive. Table 1 shows the basic statistical properties of the calculated K_{fs} and α values using the SEA procedure. Of the calculated α values, 79 out of 120 were positive. A negative value of α is physically impossible since this would mean that either K_{fs} or ϕ_m is negative. The 41 negative α values make that the overall average α of all positive and negative α values was negative. Values of α down to -10 cm^{-1} were obtained. The mean K_{fs} for locations where $\alpha > 0$ is half ($0.032 \text{ cm min}^{-1}$) of the mean K_{fs} for all locations ($0.073 \text{ cm min}^{-1}$) and only one-fifth of the mean K_{fs} where $\alpha < 0$ ($0.152 \text{ cm min}^{-1}$). Standard deviation on K_{fs} when taking only negative values into account is eight times larger than the one of K_{fs} where only positive α values are considered. Table 1 suggests that negative α values generally correspond to higher K_{fs} values. Examining the single measurements reveals that this is not true for all since distributions of K_{fs} values for positive α and for negative α overlap partly, although the overlap is minor.

As studied by Wu et al. (1993) preferential flow in macropores changes the Q_2/Q_1 ratio which may lead to negative α values. Since macropore flow is only gravity driven and barely influenced by capillary forces, the third term in Eq. (3) is very small (i.e. due to its large positive α). Therefore measurement

errors which are propagated in the intercept of the q versus H relation (sum of the first and third term), may result in a negative third term in Eq. (3) (i.e. negative α). This matches the finding of this study that locations where α is calculated negative, generally have high K_{fs} values. Preferential flow indeed increases hydraulic conductivity values (Bouma, 1981; Beven and Germann, 1982; Edwards et al., 1988; Logsdon et al., 1990). However, we will demonstrate in Section 4.2 that measurement errors result in erroneous and uncertain estimates of α values for all types of soils.

4.2. Sensitivity analysis

The aim of this part of the study is to examine the effect of small fluctuations in ‘measured’ inflow rate on K_{fs} and α . Only those observations where α was found positive using the SEA (79 locations) were used in the sensitivity analysis in order to avoid the effect of negative α values. MC simulations (1000 simulations for each of the 79 locations) result in model output statistics for K_{fs} and α . Fig. 2 shows the simulated mean value and standard deviation for K_{fs} (a) and α (b). The standard deviation of α is very high (notice the log scale) for all measurement locations and a trend of increasing standard deviation with increasing α values is observed. The sensitivity of α to small variations in inflow rate is extremely

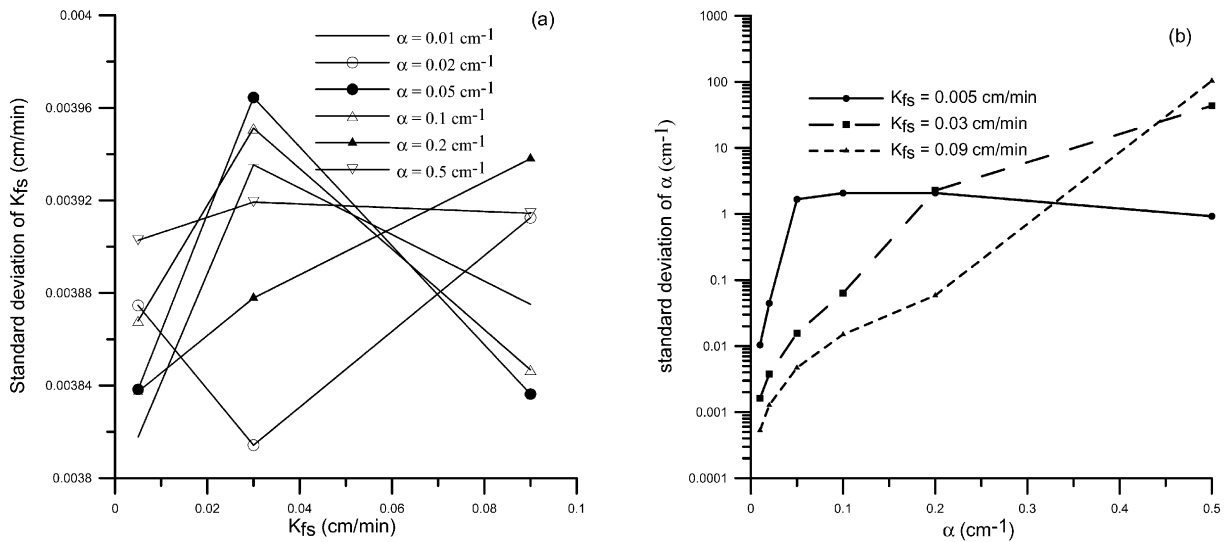


Fig. 3. Result of the MC simulations of fictive pressure head infiltrometer data using three pressure head levels (a) K_{fs} and standard deviation of K_{fs} (b) α and standard deviation of α .

high and small input fluctuations in measured infiltration rates result in a large range of α values: from -1000 up to $+2000 \text{ cm}^{-1}$. This exercise reveals that the α value calculated using the SEA from single-ring pressure infiltrometer measurements with only two pressure head levels is meaningless. This conclusion must at this stage be restricted to our conditions (e.g. initial soil moisture content and soil type, etc.). As stated earlier, negative α values do not necessarily imply high K_{fs} values (or preferential macropore flow) but as shown in the MC simulations, negative α values could also be the result of small variations in the measured infiltration rate due to e.g. measurement errors.

The standard deviation of K_{fs} is nearly constant for all measurement locations i.e. no trend of increasing standard deviation with increasing K_{fs} values can be noticed, and standard deviations remain reasonably small for all measurement locations. K_{fs} is not very sensitive to these infiltration rate measurement errors. In conclusion, single-ring pressure infiltrometer measurements using only two pressure head levels at each location is a suitable method for the in situ derivation of K_{fs} but unsuitable for estimating α .

The result of the second sensitivity analysis (three theoretical heads applied) in which three K_{fs} values (0.005, 0.03, and 0.09 cm min^{-1}) and six α values

(0.01, 0.02, 0.05, 0.1, 0.2, and 0.5 cm^{-1}) are arbitrarily chosen and MC simulations performed as explained earlier, is shown in Fig. 3. As shown in Fig. 3(a), standard deviations of K_{fs} again remain quite constant and reasonably small over the range of K_{fs} for all considered α values. Six MC simulations (1000 runs each) were performed for each of the three considered K_{fs} levels i.e. one simulation for each value of α . Fluctuations in infiltration rate over the considered range of α and K_{fs} values do not influence the standard deviation of K_{fs} . Fig. 3(b) shows that even when considering three pressure head levels, the estimated α values remain very sensitive to measurement errors in the infiltration rate over the considered range of α .

A trend of increasing standard deviation with increasing values of α can again be observed. This trend can be explained physically: low α values correspond to soils in which capillary forces are relatively important compared to gravity forces. This means that in these soils, the third term of Eq. (3) is relatively large and hence α or ϕ_m has a large influence on the value of $q_{0\infty}$. In other words, $q_{0\infty}$ is sensitive to the value of α or α can be determined quite well. On the other hand, when α increases (gravity forces more important than capillary forces), the third term becomes very small compared to the first two terms

of Eq. (3), which implies that α does not contribute a lot to the value of $q_{0\infty}$ (or $q_{0\infty}$ is insensitive to the value of α) and can hence not be determined with great certainty.

It is obvious from Fig. 3(b), that single-ring pressure infiltrometer measurements is not a suitable method to estimate α , even when using three pressure head levels. Here, the conclusion that calculated α values using SEA are meaningless can be extended to a large number of other soils having a wide range of α and K_{fs} values. Since small infiltration variations (or measurement errors) do not have a large effect on the estimation of K_{fs} , it is a stable method for the in situ estimation of K_{fs} .

4.3. Inverse optimisation technique

As discussed earlier, a single-ring pressure infiltrometer measurement is a good tool for the estimation of K_{fs} in situ. A problem remains that the estimation of K_{fs} is a function of α . However, the sensitivity analysis showed that it is impossible to obtain a meaningful estimation of α from the steady-state infiltration rate measurements. As stated earlier, Elrick et al. (1989) suggested a fixed α value method. However, individual α values for soils are generally not available.

One solution for the choice of the α value could be to consider the average of the 79 positive α values as the ‘overall’ α . Following this solution, an overall α of 0.19 cm^{-1} can be calculated. Recalculating all K_{fs} values with the overall α value would finally result in two K_{fs} values per measurement location (or 240 K_{fs}) and one overall α . Finally, the average of both K_{fs} values at each measurement location can be considered as the best estimate. However, taking the average of the positive α ’s as the overall hillslope α is not very meaningful when considering the large uncertainty in α .

An alternative, more robust way of estimating the overall α value is proposed in this study. In the sensitivity analysis, it was proven to be impossible to get an accurate estimate of local α values using the SEA. It also revealed that K_{fs} is less sensitive to measurement errors and also to an erroneous α estimate or that α can be completely out of the normal range while the estimate of K_{fs} is still acceptable. That is why the authors believe that it makes sense to suggest a fixed α for all measurement locations. Using this

fixed α value, an error is made due to the fact that the local α might differ from the optimised one but this error only has a very small impact on the estimation of the local K_{fs} .

Again, only locations where α was positive (SEA) are taken into consideration. The optimisation (Eq. (6)) aims at finding 79 a values (equivalent to 79 K_{fs} values) and 1 overall b value (related to α) by minimising the sum of the squared residuals. Several sets of initial parameters were used, all leading to the same optimised parameter set. This means that the optimised parameter set does not correspond to a local minimum in the objective function but corresponds to the overall minimum or optimum. Compared to the case in which the average of the positive α values is taken as the overall α , this optimisation procedure results in a value of α which is based on all measurements where α is positive simultaneously.

The sensitivity analysis learned that negative α values can be the result of measurement errors. Though positive α values do not imply that measurement errors are negligible, negative α values are for sure an indication of ‘large’ uncertainty, hence it makes sense (first reason) to exclude these negative α locations. It must be stressed that the actual α value using SEA is meaningless, though in this study, its sign decides whether it is to be used in the optimisation procedure or not.

When the Levenberg–Marquardt optimisation procedure was applied for all locations, including the negative α sites, the optimised α value always reached the top of the upper bound set in the optimisation procedure, even when this bound reached extreme values of 100 cm^{-1} . This is because the optimisation procedure looks for one overall α which is negative but α is not allowed to become negative by its lower bounds (set to 0). Therefore, the optimisation procedure increases the value of α in order to decrease the third term of Eq. (3) in the same way a negative α does. Hence, (second reason) the optimisation procedure was limited to the locations having a positive α value.

Fig. 4 shows the result of the optimisation procedure: simulated (‘optimised’) and measured infiltration rates are very close ($R^2 = 0.9961$) and no trend was found in the residuals. The overall α or α_{opt} was 0.03 cm^{-1} and the optimised K_{fs} values are shown in Fig. 5. The large difference between average positive

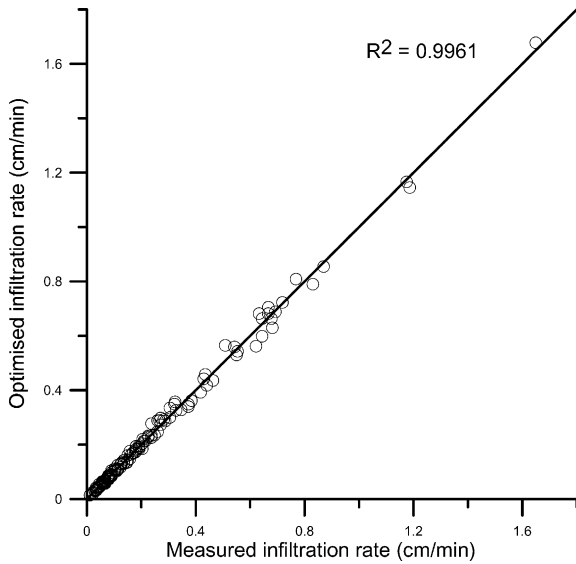


Fig. 4. Result of inverse optimisation: measured infiltration rate compared to optimised (simulated) infiltration rate.

α s using SEA (0.18 cm^{-1}) and the optimised α (0.03 cm^{-1}) is due to a few outliers (e.g. one α of 8.29 cm^{-1}) in the result of the SEA calculation and the large uncertainty on α as shown in the sensitivity analysis. Comparing this α_{opt} of 0.03 cm^{-1} with the

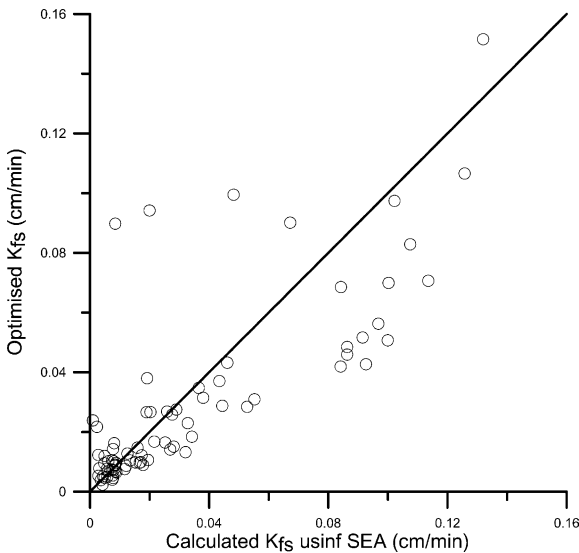


Fig. 5. Optimised K_{fs} values at locations with an originally calculated positive α compared to originally calculated K_{fs} using the SEA method.

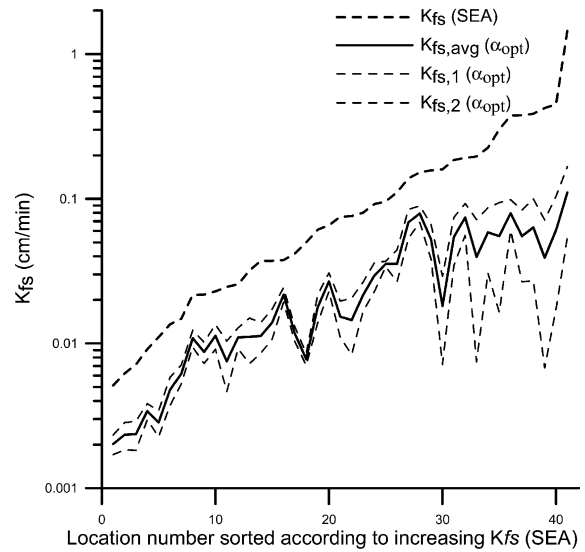


Fig. 6. K_{fs} values based on α_{opt} at locations with an originally calculated negative α .

values proposed by Elrick et al. (1989) indicates that this value lies within the range of the ‘unstructured fine textured soils’, in which the soil found at the measurement site can be classified. Optimised K_{fs} values are generally not as high as the originally calculated K_{fs} values using the SEA, although this is certainly not true for all measurement locations.

At locations where α was found negative, we solved Eq. (3) for K_{fs} using α_{opt} and obtained two K_{fs} estimates at each location, one for each applied pressure. The average of these two estimators ($= K_{fs, \text{avg}}$) is considered to be the in situ measured K_{fs} for that location. Fig. 6 shows the originally calculated K_{fs} values using the negative α , the K values from Eq. (3) for each H (using α_{opt}) and the averaged K_{fs} , which is considered to be the in situ estimated K_{fs} for that location. Fig. 6 shows that the $K_{fs, \text{avg}}$ is again lower than the originally calculated K_{fs} using negative α values, and that for all measurement locations. This is quite obvious because an increase in the third term of Eq. (3) (α from a negative to a positive value) has to be compensated by a decrease in K_{fs} for equal q values. Advantage of the optimisation technique compared to calculating K_{fs} according to SEA is that in this technique, all measurements (at least where α was found to be positive with the SEA) are involved in finding the optimum 79 K_{fs} values and the overall α

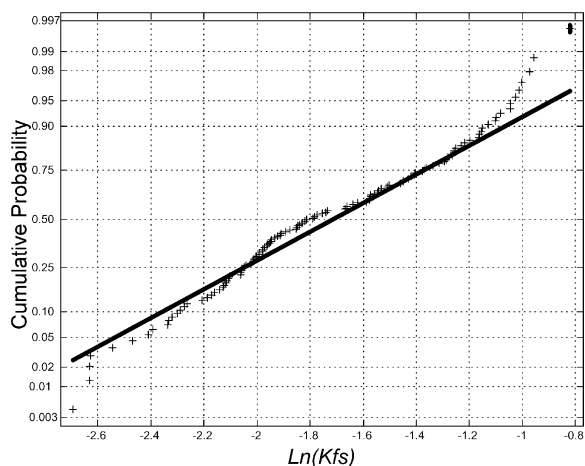


Fig. 7. Normal probability plot of $\ln(K_{fs})$. Straight line represents the theoretical cumulative normal probability function.

value simultaneously. No posterior averaging (except for the negative α values) of K_{fs} values compared to the method proposed by Elrick et al. (1989) is needed. The statistics of the K_{fs} for all locations using the overall α value are shown and compared with the K_{fs} values calculated using the SEA in Table 1.

4.4. Statistical and geostatistical results

The normal probability of the $\ln(K_{fs})$ values calculated based on α_{opt} is shown in Fig. 7. The Lilliefors test did not reject the null (normal) hypothesis at the 0.05 level of significance, meaning that K_{fs} is log-normally distributed as shown in several other studies (Jury, 1985; Russo et al., 1997; Zavattaro et al., 1999; Mohanty et al., 1994; Jacques, 2000). Fig. 8(a) shows the omnidirectional variogram of $\ln(K_{fs})$, Fig. 8(b) the directional variogram in the x -direction or orthogonal to the hillslope and Fig. 8(c) the directional variogram in the y -direction or along the hillslope. In addition, the fitted exponential model through each variogram is shown in Fig. 8. The three parameters of the exponential model (Eq. (7)) were estimated by visual fitting and are shown in Table 2. Cross-validation using the model parameters fitted to the omnidirectional variogram, resulted in a

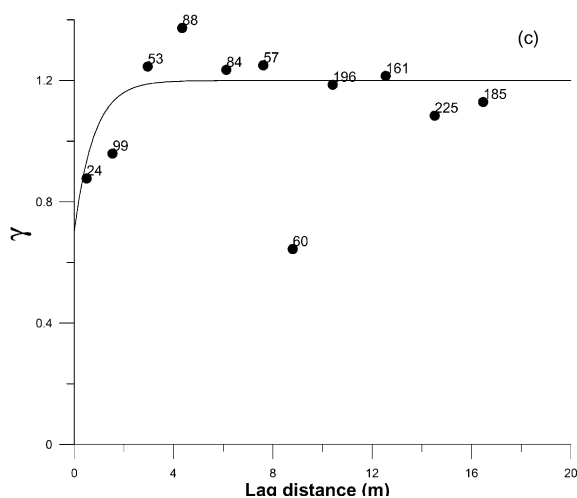
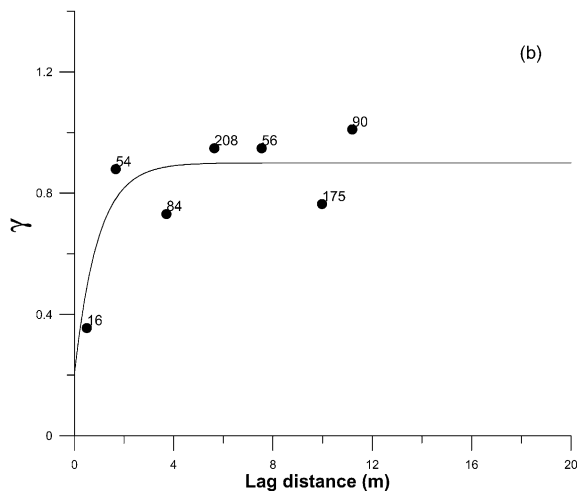
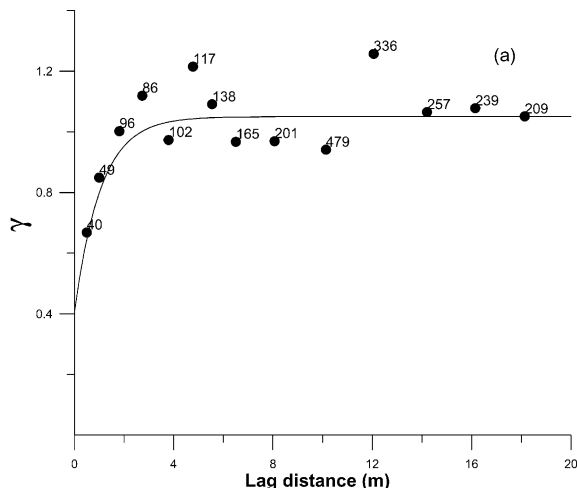


Fig. 8. Experimental semi-variograms (circles) and fitted models of $\ln(K_{fs})$ (a) omnidirectional semi-variogram (b) directional semi-variogram along x axis, and (c) directional semi-variogram along y axis.

mean of the reduced error vector (ME) of -0.045 , a mean square reduced error (MRE) of 1.056 . As these values are ideally, respectively, 0 and 1 , the fitted model was found to be suitable.

Examining the semi-variograms reveals that some spatial pattern is present in all the three semi-variograms. A range of $\ln(K_{fs})$ of 2.85 m (omnidirectional) to 3.8 m (along the hillslope) is observed. Russo et al. (1997) found a range of $\ln(K_{fs})$ between 0.6 and 2.5 m which is in the same order of magnitude as the values found here. The quite high nugget values also suggest that the local variation between adjacent locations is high. As shown earlier, the uncertainty of measurement errors on the K_{fs} is reasonably small, so this rather short correlation distance or range could be caused by several other factors. The field plot used to be a fruit tree orchard of which the roots have created preferential flow pathways resulting of course in the shortening of the range. Worm- or moleholes can be another factor resulting in big differences between adjacent measurements.

5. General conclusions

In situ measurements of discharge–head (Q – H) pairs were used to estimate the field-saturated hydraulic conductivity K_{fs} , and the parameter α (Gardner, 1958) at 120 locations on a hillslope (80 m long, 20 m wide) by means of a single-ring pressure infiltrometer. Only the steady-state infiltration rate was used for further analysis and using the classical SEA approach, 79 of these (Q , H) pairs yielded positive α while all pairs resulted in positive K_{fs} values. The SEA approach showed that locations where α was negative, generally have high K_{fs} values. The negative α values might be the result of the domination of macropore flow in the infiltration process at that location, though negative α values do not imply that preferential macropore flow (or higher K_{fs}) is the case as

Table 2
Estimated parameters of the exponential semi-variogram models

	Nugget (C_0)	Sill (C_s)	Range in m (a)
Omnidirectional	0.4	0.65	2.85
Directional (x)	0.2	0.7	3.2
Directional (y)	0.7	0.5	3.8

shown in the sensitivity analysis. This MC analysis reveals that the sensitivity of α on measurement errors using the constant head SEA with two or three pressure head levels is enormous. Therefore, negative α values can be the result of a small measurement error instead of macropore flow. Sensitivity of K_{fs} to measurement errors is very low and constant over the range of K_{fs} and α . Based on this sensitive analysis, we believed that single-ring pressure infiltrometer measurements using two or three pressure head levels at each location is a suitable method for the in situ derivation of K_{fs} but unsuitable for the estimation of α .

A new technique using the inverse optimisation of 120 K_{fs} values and only one α value using all infiltration measurements was proposed. The technique allows a robust method for the derivation of that α value which is generally not known for a given location. The inverse optimisation converged successfully and optimised and measured infiltration rates are very close. Finally, the spatial analysis revealed ranges of $\ln(K_{fs})$ between 2.85 and 3.8 m omnidirectional and along the hillslope (y -axis), respectively.

Acknowledgements

We would like to thank the Fund for Scientific Research Flanders (Belgium) (F.W.O.-Vlaanderen) as the corresponding author is a Research Assistant of the Fund for Scientific Research Flanders. A well meant thanks to Seyoum Assefa Terefe for the assistance in the measurements.

References

- Angulo-Jaramillo, R., Vandervaere, J.P., Roulier, S., Thony, J.L., Gaudet, J.P., Vauclin, M., 2000. Field measurement of soil surface hydraulic properties by disc and ring infiltrometers. A review and recent developments. *Soil Tillage Res.* 55, 1–29.
- Ankeny, M.D., Ahmed, M., Kaspar, T.C., Horton, R., 1988. Design for automated tension infiltrometer. *Soil Sci. Soc. Am. J.* 552, 893–896.
- Bagarello, V., Provenza, G., 1996. Factors affecting field and laboratory measurements of saturated hydraulic conductivity. *Trans. ASAE* 39, 153–159.
- Bard, Y., 1974. *Non-linear Parameter Estimation*. Academic Press, San Diego, CA.
- Beven, K., Germann, P., 1982. Macropores and water flow in soils. *Water Resour. Res.* 18, 1311–1325.

- Bouma, J., 1981. Soil morphology and preferential flow along macropores. *Agric. Water Manag.* 3, 235–250.
- Conover, W.J., 1980. *Practical Nonparametric Statistics*. Wiley, New York.
- Cressie, N.A.C., 1993. *Statistics for Spatial Data*. Wiley, New York 900 p.
- Deutsch, C., Journé, A., 1992. *GSLIB, Geostatistical Software Library and User's Guide*. Oxford University Press, New York 340 p.
- Edwards, W.M., Norton, L.D., Redmond, C.E., 1988. Characterising macropores that affect infiltration into non-tilled soil. *Soil Sci. Soc. Am. J.* 52, 483–487.
- Elrick, D.E., Reynolds, W.D., 1992. Methods for analyzing constant head well permeameter data. *Soil Sci. Soc. Am. J.* 56, 320–323.
- Elrick, D.E., Reynolds, W.D., Tan, K.A., 1989. Hydraulic conductivity measurements in the unsaturated zone using improved well analyses. *Ground Water Monit. Rev.* 9, 184–193.
- Elrick, D.E., Parkin, G.W., Reynolds, W.D., Fallow, D.J., 1995. Analysis of early-time and steady state single-ring infiltration under falling head conditions. *Water Resour. Res.* 31, 1883–1893.
- Elrick, D.R., Reynolds, W.D., 1992. Advances in measurement of soil physical properties: bringing theory into practice. *SSSA Spec. Publ.* 30, 1–24.
- Gardner, W.R., 1958. Some steady state solutions of unsaturated moisture flow equations with application to evaporation from a water table. *Soil Sci.* 85, 228–232.
- Heinen, M., Raats, P.A.C., 1990. Evaluation of two models describing the steady discharge from a constant head well permeameter into unsaturated soil. *Soil Sci.* 150, 401–412.
- Jacques, D., 2000. Analysis of water flow and solute transport at the field scale. PhD Thesis nr. 454. Faculty of Agricultural and Applied Biological Sciences, K.U. Leuven, Belgium, 255 p.
- Journé, A.G., Huijbregts, C., 1978. *Mining Geostatistics*. Academic Press, New York.
- Jury, W.A., 1985. Spatial variability of soil physical parameters in solute migration: a critical literature review. EPRI EQ-4228 Project 2485-6, Riverside, CA.
- Jury, W.A., Russo, D., Sposito, G., Elabd, H., 1987a. The spatial variability of water and solute transport properties in unsaturated soil. I. Analysis of property variation and spatial structure with statistical models. *Hilgardia* 55, 1–32.
- Jury, W.A., Russo, D., Sposito, G., Elabd, H., 1987b. The spatial variability of water and solute transport properties in unsaturated soil. II. Scaling models of water transport. *Hilgardia* 55, 33–56.
- Logsdon, S.D., Allmaras, L., Wu, L., Swann, J.B., Randall, G.W., 1990. Macroporosity and its relation to saturated hydraulic conductivity under different tillage practices. *Soil Sci. Soc. Am. J.* 54, 1096–1101.
- Mohanty, B.P., Ankeny, M.D., Horton, R., Kanwar, R.S., 1994. Spatial analysis of hydraulic conductivity using disc infiltrometers. *Water Resour. Res.* 30, 2489–2498.
- Philip, J.R., 1985. Approximate analysis of the borehole permeameter in unsaturated soil. *Water Resour. Res.* 21, 1025–1033.
- Reynolds, W.D., Elrick, D.E., 1990. Pondered infiltration from a single ring. Part 1. Analysis of steady flow. *Soil Sci. Soc. Am. J.* 54, 1233–1241.
- Reynolds, W.D., Elrick, D.E., Topp, G.C., 1983. A reexamination of the constant head well permeameter method for measuring saturated hydraulic conductivity above the water table. *Soil Sci.* 136, 250–268.
- Reynolds, W.D., Elrick, D.E., Clothier, B.E., 1985. The constant head well permeameter: effect of unsaturated flow. *Soil Sci.* 139, 172–180.
- Russo, D., Jury, W.A., 1987a. A theoretical study of the estimation of the correlation scale in spatially variable fields. 1. Stationary fields. *Water Resour. Res.* 23, 1257–1268.
- Russo, D., Jury, W.A., 1987b. A theoretical study of the estimation of the correlation scale in spatially variable fields. 2. Nonstationary fields. *Water Resour. Res.* 23, 1269–1279.
- Russo, D., Russo, I., Laufer, A., 1997. On the spatial variability of parameters of the unsaturated hydraulic conductivity. *Water Resour. Res.* 33, 947–956.
- Stephens, D.B., Lambert, K., Watson, D., 1987. Regression models for hydraulic conductivity and field test of the borehole permeameter. *Water Resour. Res.* 23, 2207–2214.
- Vauclin, M., Elrick, D.E., Thony, J.L., Vachaud, G., Revol, Ph., Ruelle, P., 1994. Hydraulic conductivity measurements of the spatial variability of a loamy soil. *Soil Technol.* 7, 181–195.
- Wu, L., Swan, J.B., Nieber, J.L., Allmaras, R.R., 1993. Soil-macropore and layer influences on saturated hydraulic conductivity measured with borehole permeameters. *Soil Sci. Soc. Am. J.* 57, 917–923.
- Zavattaro, L., Jarvis, N., Persson, L., 1999. Use of similar media scaling to characterise spatial dependence of near saturated hydraulic conductivity. *Soil Sci. Soc. Am. J.* 63, 486–492.